Energy 283 (2023) 128453

Contents lists available at ScienceDirect

Energy

journal homepage: www.elsevier.com/locate/energy

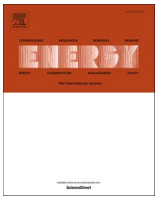

Energy efficiency and thermal comfort of buildings in arid climates employing insulating material produced from date palm waste matter

Djamel Belatrache [a], Said Bentouba [b], Nadjet Zioui [c], Mahmoud Bourouis [d,*]

[a] Laboratory of Promotion and Valorization of Saharan Resources (VPRS), University Kasdi Merbah, 30000, Ouargla, Algeria
[b] NORCE, Norwegian Research Centre, Prof. Olav Hanssensvei 15, 4021, Stavanger, Norway
[c] Mechanical Engineering Department, University of Quebec at Trois-Rivieres, QC, Canada
[d] Department of Mechanical Engineering, Universitat Rovira i Virgili, Av. Països Catalans No. 26, 43007, Tarragona, Spain

ARTICLE INFO

Handling Editor: X Ou

Keywords:
Thermal conductivity
Natural insulation
Date palm material
Building heat loss
Arid climate

ABSTRACT

This study investigates the suitability of using waste material from date palm trees in thermal insulation for buildings in arid climates. Thermal conductivity was experimentally determined from a few samples of bricks containing recycled date palm fiber (DPF) and date palm spikelet (DPS). Among the samples investigated, the one containing 1.36% DPS in weight demonstrated the best characteristics for insulation purposes yielding a thermal conductivity of 0.106 W/m.K. Theoretical and experimental investigations were carried out on walls and roofs built using DPS and DPF material to see what impact it would have on energy efficiency and thermal comfort. The electricity consumption for cooling decreased by up to 64.7% and 41.2%, during the summer months, for DPS and DPF, respectively, compared to buildings erected with sand and clay. It was also concluded that the greatest amount of thermal energy entering the rooms takes place through the roofs. Four roof-materials were tested, namely: Polystyrene, Air gap, DPF, and DPP on three different days. As a thermal insulator, DPF demonstrated the best thermal comfort conditions; polyester yielded poorer thermal comfort conditions and DPP delivered rather weak results.

1. Introduction

Environmental pollution is largely caused by the irrational use of fossil fuels to produce electrical energy and the dependency of power generation on the combustion of fossil fuels. This practice causes emissions of huge amounts of carbon dioxide (CO2) into the atmosphere and subsequent global warming. In the building sector, greenhouse gas (GHG) emissions are mainly due to the high consumption of electricity by equipment used for air-conditioning i.e., cooling and heating to maintain thermal comfort. The high consumption of energy is the result of the significant heat exchange between the interior and exterior of the building. One of the challenges would be to significantly reduce energy consumption by using locally available insulating materials for building [1].

If thermal insulation materials are incorporated into building practices in hot climates, it could reduce the high consumption of electricity in summer when the daily temperatures climb to over 40 °C and continue for a long period [2,3]. Materials such as fibers, petioles, and spikelets derived from date palm waste matter could be used as additives in composite construction materials. Among the advantages gained from adding these materials are features like, renewability, low cost, availability, absence of toxicity and polluting effects. In addition, these materials ensure good thermal performance for mechanical and thermal insulation [4–6].

Mawardi et al. [7] conducted an examination of oil palm wood-based bio-insulation materials, with special focus on heat conductivity, mechanical properties, and physical characteristics. They also investigated how hybridization and particle size influenced the properties of the panels. Their findings revealed that both hybridization and particle size significantly impacted the panel properties. The density of the panels ranged from 0.66 g/cm^3 to 0.79 g/cm^3, while the thermal conductivity varied between 0.067 W/m.K and 0.154 W/m.K. The hybrid panels with coarse particles and a density of 0.66 g/cm^3 exhibited the lowest thermal conductivity at 0.067 W/m.K.

This effect was however, partly cancelled out by the increase in vapour pressure. It was reported in the literature [8], that building materials derived from vegetable fibers offer a good solution for optimizing energy consumption in those buildings that do not suffer environmental impacts i.e., toxicity and greenhouse gas emissions. Awad

* Corresponding author.
E-mail address: mahmoud.bourouis@urv.cat (M. Bourouis).

https://doi.org/10.1016/j.energy.2023.128453
Received 20 April 2023; Received in revised form 6 July 2023; Accepted 15 July 2023
Available online 18 July 2023

Nomenclature

A	Surface area (m^2)
Cp	Specific heat capacity of the soil (J/kg.K)
L_s	Thickness (m)
I	Total solar radiation on the horizontal surface (W/m^2)
h	Convective heat transfer coefficient ($W/m^2.K$)
q	Heat flux (W/m^2)
R	Thermal resistance ($m^2.K/W$)
V	Volume (m^3)
Q	Heat flow (W)
T	Temperature (°C)
t	Time (Hour)
Qcool	Average daily cooling potential (Wh)

Subscripts

Amb	Ambient
DPF	Date palm fibers
DPS	Date palm spikelet
DPP	Date palm petiole
In	Indoor
Out	Outdoor
Int	Internal surface
Ext	External surface
Poly	Polystyrene

Greek letters

λ	Thermal conductivity (W/m.K)
ρ	Density of sample (kg/m^3)
η	Mean efficiency of system (%)

et al. [9] centered their research on the fibers of the date palm tree, and included exploring their origins, characteristics, treatments, and developments in composite materials. They established a comprehensive database and platform for effectively utilizing date palm fibers for the production of sustainable and renewable materials, particularly to develop date palm fiber composites for various applications.

In a separate study, Awad et al. [10] examined how the diameter size and loading content of date palm fibers (DPF) could impact the mechanical and physical properties of recycled polyvinyl chloride (RPVC) composites that were reinforced with DPF. The composites were prepared through a melt-mixing process followed by compression molding. At a weight percent of 40 DPF, the tensile strength (TS), moisture content (MC), and water absorption (WA) showed the highest results, with increased values of 1.57%, 1.76%, and 10.80%, respectively. Different applications may require specific densities and bonding agents. In another study, Awad et al. [11] explored the effects of DPF density, diameter size, and content on the mechanical and physical properties of a bio-composite reinforced with polylactic acid (PLA). The bio-composites were prepared through a melt-mixing process and subjected to compression molding. Tensile, flexural, and impact strengths were evaluated, and parameters such as thickness swelling (TS), moisture content (MC), and water absorption (WA) were assessed. At 40 weight percent DPF, the TS, MC, and WA exhibited the greatest increases, with values of 4.10%, 4.9%, and 8.2%, respectively. The study also employed SEM analysis to examine the interfacial bonding between PLA matrix and DPF. Although the mechanical properties decreased as the DPF content increased (depending on the geometry of the DPF), the findings indicate that these technologies have potential for commercialization in non-structural applications as part of a waste management system. Elseify et al. [12] conducted a comprehensive review of the literature on date palm fibers, covering extraction methods, properties, and applications. This review provides a valuable resource for researchers as it highlights existing knowledge gaps and offers insights into how to use date palm fibers for creating new materials. Furthermore, Kaczynski et al. [13] investigated how phase change materials (PCM) and conventional masonry could impact on the summertime thermal performance of a non-air-conditioned residential building in a temperate region. Three rooms with different walls and ceiling structures were studied. The study found that traditional high thermal capacity building materials were more effective than PCMs in reducing high indoor temperatures during summer. Ng et al. [14] employed the life cycle energy assessment approach to investigate the trade-offs between EE production and OE savings for five different types of insulation envelopes and evaluate the EE and OE of non-green and green-rated non-residential buildings with hotspot analysis. According to the findings, Embodied energy accounts for 16–19% of all energy in both non-green and green-rated non-residential buildings; as a result, Embodied energy shouldn't be overlooked in the green building certification system. Additionally, insulated building envelopes reduce cooling demand by 84–87% compared to non-insulated walls, with cellulose fiber insulators using the least energy. Damfeu et al. [15] obtained the thermophysical properties of composite building materials, cinder blocks of pozzolans and cinder blocks of sand. The results showed that pozzolan cinder blocks demonstrated lower thermal conductivity and higher volumetric heat capacity than those of sand cinder. Mastouri et al. [16] investigated the effect of combining thermal insulation and high thermal inertia of a house located in the Green City of Benguerir in Morocco. The authors compared two buildings, in the former, local materials with passive and hybrid cooling techniques were employed, while the latter incorporated classic construction materials. The results showed that the minimum indoor air temperature was up to 5 °C higher in winter, while the maximum indoor air temperature was reduced by up to 9 °C in summer. The annual cooling and heating load of the building was reduced by up to 81% less than that of the classic construction. Korjenic et al. [17] presented the effect of natural fiber insulation materials on hydrothermal comfort buildings. Three types of fibers were selected for initial determination of the properties: fibers from jute, flax, and technical hemp. The results indicated that the thermo-insulating materials derived from natural resources are sensitive to the humidity of the structure they are built of.

In livestock housing, mechanical ventilation systems are frequently used to reduce indoor air pollution and regulate the temperature. The systems need to be properly controlled during operation in accordance with changes in the indoor and outside thermal settings [18]. The roofs are proving very effective in reducing energy requirements for cooling in buildings and electricity demands peak. Several researchers have investigated how the shape of the roof and the components used affect the internal room temperature [19]. Moreover, significant experimental and numerical investigations were carried out to assess the efficiency of cool-roofs in different climatological conditions. Macintyre and Heaviside [20] investigated the potential benefits of employing cool-roofs to reduce heat-related mortality occurring during heatwaves suffered in a European city. The results indicated that the urban heat island effect was most pronounced at nighttime, and the effect of cool-roofs was most significant in the daytime. Average daytime temperatures were reduced by 0.5 °C, and up to a maximum decrease of ~3 °C was registered when this system was implemented in commercial/industrial a reas. Mungur et al. [21] evaluated the efficiency of the green-roof system, which is gauged by how it affects indoor temperature fluctuations, conductive heat fluxes and daily peak indoor temperatures. The maximum heat flux on each day ranged from 0.4797 to 2.5190 W/m^2 for a conventional roof and from 0.2090 to 0.5312 W/m^2 for a green-roof. The authors concluded that both in mid-winter and late winter, the green-roof significantly decreased heat loads in comparison to a conventional

roof. Abdelaziz et al. [22] conducted a comprehensive analysis combining numerical simulations and experimental investigations to evaluate the mechanical behavior of mortar modified with palm fronds. One of the main objectives was to determine whether the effect of palm fibers acted as a filler or a reinforcement. Additionally, the study aimed to quantify the interfacial effect, which had previously been proposed qualitatively but lacked sufficient mechanistic support. The results indicated that the inclusion of untreated palm spikelets as a volume reinforcement of 1% showed a negligible impact on the performance of the mortar compared to the reference mixture. However, adding higher contents of palm spikelets resulted in a significant degradation of mechanical performance. The introduction of carbon nanotubes (CNT) partially enhanced performance, and treating spikelets chemically with NaOH and CaO also strengthened action. The numerical predictions for formulations incorporating small palm spikelets, CNT, and chemical treatment, demonstrated a constrained load transfer across the interface between the matrix and the untreated spikelets, which indicates substantial interface stiffness.

Stavrakakis et al. [23] investigated how cool-roofs affected thermal and energy performance in a school building located in Athens, Greece. The results of an experimental and numerical assessment of the impact of a cool-roof indicated that the hourly indoor air temperature below a cool-roof was 1–2.6 °C lower in July. Measured on a warm summer day, the predicted mean value (PMV) used to indicate thermal comfort was at least 24% lower in the building with the cool-roof, and energy consumption for cooling was at least 18% less. Qin et al. [24] modelled the daily accumulation of heat moving inwards from building roofs with different albedo values. They correlated the heat gain in the building roof to both the rooftop albedo and the incident solar radiation. A small building cell was constructed to monitor the heat gained in the building by using both a non-insulated and an insulated roof. It was found that roof insulation increased in the rooftop albedo, and that both options could effectively curtail the heat gain in buildings during the summer season. Suarez et al. [25] evaluated the thermal performance of a single-family house located in a coastal city in northern Spain. The authors reported that the ventilation systems and thermal insulation could be 81% and 57% respectively, lower than in the case of a standard type of house.

Brito Filho and Oliveira Santos [26] analyzed the thermal performance of large metal roofs in equatorial climate regions in Brazil. The authors presented a comparative analysis of the thermal performance of large metal roofs like those found on exhibition halls, airports, and malls, located in subtropical and equatorial climate regions in Brazil. The results showed that the roof with the thermal insulation layer and selective coating was the best option in cities with an equatorial climate in terms of energy saving and mitigating the impact of the urban heat island phenomenon. In cities with a subtropical climate, the application of white paint, on a roof that lacked a thermal insulation layer, was the best solution for both a reduction in energy consumption and a decrease in the formation of an urban heat island.

Vera et al. [27] presented a parametric analysis to evaluate how vegetable fiber roofs could affect the cooling and heating demands of a big-box in different semi-arid and marine climates, namely Albuquerque (USA), Santiago (Chile) and the marine climate of Melbourne (Australia). The authors reported that vegetation could be more effective than insulation to reduce cooling loads. This was due to the evapotranspiration of the vegetation-substrate system and the canopy shade. They also concluded that thermal insulation influenced the stand-alone retail heating loads more than what the substrates and leaf area index (LAI) of vegetation did.

For thermal insulation in building, Nocentini et al. [28] investigated handy, light, super-insulating aerogel blanket material, dried in ambient conditions. Two types of blankets were considered: the former had a glass fiber web and the latter, a polyethylene terephthalate (PET) web. Hygro-thermal characterizations carried out showed that the aerogel blankets demonstrated excellent thermal conductivity (0.015 W/m.K) and hydrophobic behavior. Aerogel blankets obtained using a new ambient drying process, showed practically the same characteristics as their counterparts, dried by a supercritical process, and hence, marked a step forward in aerogel blanket industrialization.

Kadri et al. [29] investigated the contribution of a double skin roof, coated with thermo-reflective paint, to improve thermal and energy performance for the 'Mozabit' houses. The house case study in question, was located in the Ksar of Beni Isguen in southern Algeria. The authors reported that in summer, the temperatures in traditional houses were higher than tolerated for comfort. The investigation period contemplated three days representative of the hot season; the average indoor operating temperatures exceeded 37 °C at different hours of the day. They concluded that the approach they proposed had decreased the indoor temperature by almost 5 °C. Moreover, the overall energy consumption required for cooling loads was reduced by 572 kWh i.e., 66% hence optimizing the thermal performance of the roof.

Bovo et al. [30] focused their investigation on the use of corn cob fiber, as a natural insulation material for use in buildings. Experimentally, they assessed at both micro and macro scale, specific heat, thermal conductance, thermal conductivity, and the sound reduction index. Specific heat ranged from 1.4 to 1.9 kJ/kg.K, while density was around 200 kg/m^3, and thermal conductivity varied between 0.14 and 0.26 W/m.K. The authors suggested evaluating natural materials for building construction applications.

He et al. [31] evaluated the plant evapotranspiration (ET) effect on green-roofs in tropical areas. A field experiment was conducted to quantify the ET rate of four plant species in Singapore. Basic plant properties were measured for four green-roof types in Singapore. The authors reported that the average daytime rate of ET ranged from 198.4 to 320 g/m^2.h, while the average nighttime rate of ET ranged from 18.7 to 25.5 g/m^2.h. The percentage of daytime ET accounting for solar radiation ranged from 51.4% to 62.7%.

With a view to the conservation of global energy resources, Ozarisoy et al. [32] reviewed the extant literature on bio-climatic design systems. They explored the ways in which specific passive-cooling design strategies could be used to optimize thermal comfort and acclimatize indoor-air environments for the occupants. To demonstrate the feasibility of applying vernacular passive-cooling design strategies in building envelopes, the authors investigated the thermal performance of prototype vernacular buildings to ascertain the efficiency of passive design systems.

Lee et al. [33] reported on the impact of external insulation and internal thermal density upon energy consumption in buildings in a temperate climate with four distinct seasons. They reviewed how energy consumption for heating and cooling in buildings would be affected by strengthening the degree of external insulation and what degree of internal heat gain would be achieved. Using parametric simulation methods, they analyzed the variation in energy consumption for annual heating and cooling purposes and collated this with the diverse levels of internal heat gain and envelope properties. The authors concluded that on increasing the degree of insulation, less total energy was required for heating and cooling in buildings with low levels of internal heat gain, while more energy was required in large office buildings with high levels of internal heat gain.

In his PhD thesis, Belatrache [34] investigated the impact of using local palm waste matter, in the envelope of a house in southern Algeria. The objective was to improve indoor thermal comfort and reduce electricity consumption. He concluded that by using local waste materials as thermal insulators energy consumption could be significantly reduced.

The main objective of this research is to evaluate the impact on the energy performance of buildings in hot climates of using thermal insulation made from waste date palm matter. First, the thermal conductivity of seven brick samples made with different materials and concentrations was experimentally determined. Afterwards, a thermal and energy analysis was carried out of three different types of rooms. These rooms had incorporated the most performant insulators that had

Fig. 1. Picture of composite sample: (a) Sand, clay, and date palm fibers; (b) Sand, clay, and date palm spikelet; (c) Mold dimensions.

Table 1
Proportions of the samples tested and their calculated density.

Sample	Sand (kg)	Clay (kg)	DPF (g)	DPS (g)	Final weight (kg)	Density (kg/m^3)
(a)	6.4	1.6	0	0	7.576	1957.6
(b)	6.4	1.6	0	50 g	7.166	1851.7
(c)	6.4	1.6	0	75 g	7.722	1995.3
(d)	6.4	1.6	0	100 g	7.326	1893.0
(e)	6.4	1.6	50 g	0	6.940	1793.0
(f)	6.4	1.6	75 g	0	7.400	1912.0
(g)	6.4	1.6	100 g	0	7.550	1950.9

been determined in the previous step into the walls and roofs. The suitability of using date palm waste matter as thermal insulation in the construction of buildings in those regions would represent both an economical solution for energy costs, and a sustainable approach in development.

2. Thermophysical properties of the materials

In this paragraph, the type and quantity of the materials which were used to build the seven samples are described. Moreover, the method used to dry the samples, and the experimental procedure employed to determine the thermal conductivity are also presented. The main results are then presented and discussed.

2.1. Determination of the thermal conductivity

2.1.1. Sample preparation

The materials used to prepare the samples consisted of a pure soil from Adrar, clay powder and two other types of local materials i.e., fibers and spikelets extracted in different proportions from the palms. All these materials came from the surroundings of the local township of Adrar, located in the southwest of Algeria. The sample preparation was carried in the laboratory with the following procedures: 6.4 kg (80%) net sand and 1.6 kg (20%) of clay were ground and then mixed for 4–5 min to obtain a homogeneous mixture. A quantity of water was added to make the mixture more cohesive and after this, local materials were added at different rates and proportions. The dough was packaged with hand pressure to make it more compact and placed in a mold with internal dimensions of 300 x 300 × 40 mm as shown in Fig. 1. Afterwards, the samples were stored for 7–10 days to get rid of any water and become a brick, ready for the experiment. Table 1 presents the proportion of material used in each sample.

Several previous tests had been carried out to obtain the optimum proportions of materials that would maintain the shape and consistency of the piece. The proportions shown in Fig. 2 showed the best results, namely DPS at 0.70%, 0.97% and 1.36% in weight and DPF at 0.72%, 1.01% and 1.32% in weight. The thermal conductivity of these samples was determined experimentally.

2.1.2. Experimental and calculation procedures

The thermal conductivity of the different samples was determined with a commercial experimental unit that uses a PID controlled flat plate electrical heater and a water-cooled flat plate with an integrated and highly sensitive heat flowmeter (Fig. 3(a)). A stationary method, based on international standard ISO 8301, was employed in this study [35]. The sample being tested was placed between a hot plate and a thermal flow metre, which was attached to a cold plate (Fig. 3(b)). The hot and cold plates were maintained at temperatures of 40 °C and 24.5 °C, respectively. The optimum temperature difference between the hot and cold plates was between 15 °C to 20 °C. The maximum temperature allowed for the hot plate was 100 °C. The time required to reach a stationary state depends on the materials in the sample and the inertia of the cooling circuit. Materials with good insulation characteristics take longer than the ones with low insulation characteristics. Experiments carried out in the present work took between 4 and 6 h.

After drying the samples for about 10 days, each sample was weighed and calculated the density was calculated using the following equation:

$$\rho = M/V \tag{1}$$

The thermal conductivity of the sample was obtained from a correlation given by the manufacturer of the experimental unit. This correlation uses the data measured together with those calibration constants given by the manufacturer. Then, the thermal resistance of each sample was calculated by the following expression:

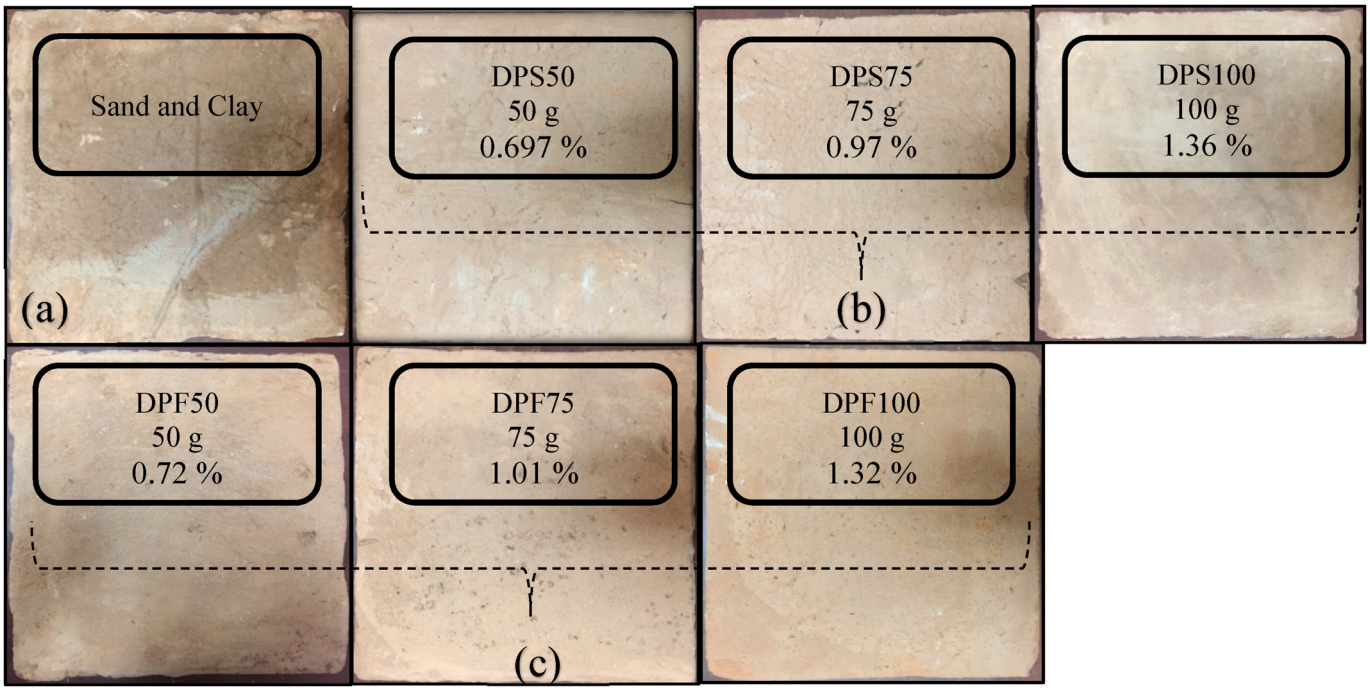

Fig. 2. Samples employed to determine the thermal conductivity: (a) Without date palm; (b) With date palm spikelet (DPS); (c) With date palm fiber (DPF).

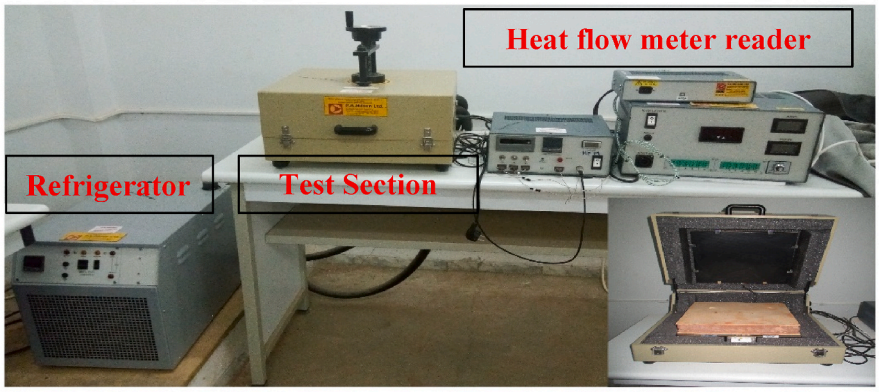

(a)

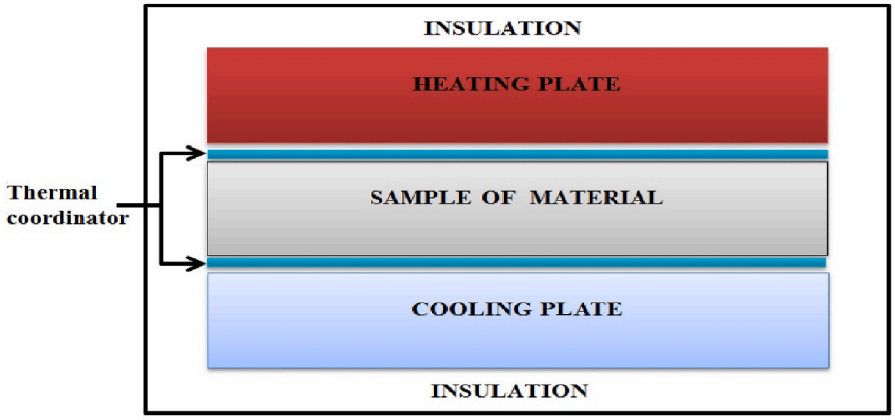

(b)

Fig. 3. (a) Main components of the experimental unit; (b) Test section.

$$R = \frac{e}{\lambda} \quad (2)$$

Table 2
Thermal conductivity of the samples tested.

Samples	DPF (%)	DPS (%)	λ (W/m.K)
(a)	0	0	1.870
(b)	0.72	0	0.742
(c)	1.01	0	0.683
(d)	1.32	0	0.381
(e)	0	0.697	0.130
(f)	0	0.97	0.129
(g)	0	1.36	0.106

2.2. Experimental data of density and thermal conductivity

2.2.1. Density

The density of the sample varies depending on the density of all the individual constituents involved, i.e., entrapped air, DPS-DPF ratio and the maximum size of aggregate. Results of the freshly mixed densities are reported in Table 1. Samples including DPF or DPS showed a lower density than the samples composed of only sand and clay. There is not a clear trend in density variation as the content of DPF or DPS increases.

2.2.2. Thermal conductivity

The experiment using the thermal flow meter method was repeated more than seven times on each sample to estimate the measurement error and obtain an average value of thermal conductivity. The thermal conductivity of the samples investigated, is presented in Table 2. Fig. 4 illustrates the effect of content of the additive on thermal conductivity for both materials used. It may be noted that thermal conductivity decreases as the content of DPF or DPS increases. The thermal conductivity of the sample without any additives is 1.87 W/m.K. It is worthy of note that the effect of DPS on the insulation characteristics of the sample is significant. Among the samples investigated, the one containing DPS at 1.36% in weight, demonstrated the best insulation characteristics with a thermal conductivity of 0.106 W/m.K. The results also showed that the use of DPF as an additive in the basic insulator composed of sand and clay was less effective even though it proved to be a good insulator. The effect of the additives (DPF or DPS) and their contribution (%wt.) is shown graphically in Fig. 4.

3. Dynamic thermal analysis using three types of date palm-based construction materials in rooms in arid climates

In this section, a dynamic thermal analysis of three different rooms was carried out to check how energy performance in buildings was affected when using thermal insulation made of date palm matter. The aim was to demonstrate how effective these materials are for thermal insulation and how they improve thermal comfort in rooms. The investigation determined which surfaces i.e., walls and roofs were more influenced by solar irradiation. The analysis was carried out using the TRNSYS simulation tool for one day per month of the summer period, i.e., July, August, and September.

3.1. Description of the simulation model

The simulation of the system was conducted using the TRNSYS environment, and specifically utilizing the "Multi-zone Building" Type 56 developed by XYZ Corporation in the United States [36]. To incorporate meteorological data from the Adrar township, subroutine Type 109-TMY2 was employed. An essential component of this simulation was TRNBuild, a software tool developed by the German Solar Energy Lab. The main input data to the multi-zone building model were the geometric and material characteristics and the control strategies of the cooling system [37]. In the present work, three rooms, built with three different types of bricks were investigated, as shown in Fig. 5. None of the rooms had any internal energy loads and all three had the same roof type, floor type, one window, and a door. Each had different walls in terms of constituent materials, namely (a) simple clay brick; (b) clay brick with DPF; (c) clay brick with DPS. The contain of the additive

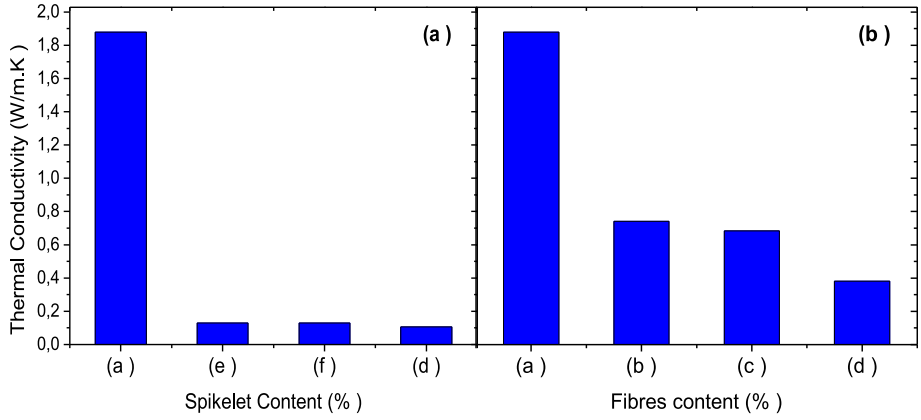

Fig. 4. Effect of the content of the additive (% in weight) on thermal conductivity: (a) Date palm spikelet (DPS); (b) Date palm fiber (DPF).

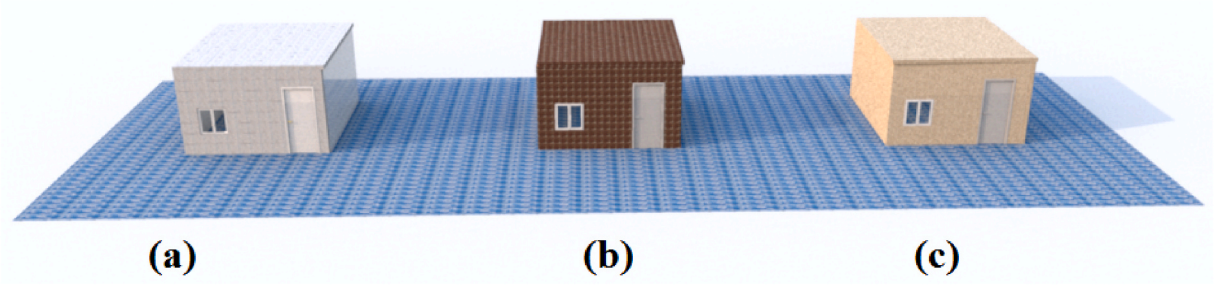

Fig. 5. Schematic diagram of the three rooms investigated: (a) Simple clay brick; (b) Clay brick with date palm fiber, (c) Clay brick with date palm spikelet.

Table 3
Thermal characteristics of the materials used in each room.

	Unit	Room (a)			Room (b)			Room (c)		
Walls	–	Sand & Clay	Plaster	Gypsum	W_{DPF}	Plaster	Gypsum	W_{DPS}	Plaster	Gypsum
	λ (W/m.K)	1.869	1.389	0.210	0.381	1.389	0.210	0.106	1.389	0.210
	e (m)	0.240	0.015	0.012	0.240	0.015	0.012	0.240	0.015	0.012
	R ($K.m^2/W$)	0.128	0.011	0.057	0.630	0.011	0.057	2.264	0.010	0.057
Roof	–	Sand & Clay		INSUL	DPF		INSUL	DPS		INSUL
	λ (W/m.K)	1.869		0.040	0.381		0.040	0.106		0.040
	e (m)	0.240		0.160	0.240		0.160	0.240		0.160
	R ($K.m^2/W$)	0.128		4.000	0.630		4.000	2.264		4.000
Ground			Floor		Stone			Concrete		INSUL
	λ (W/m.K)		0.070		1.389			2.100		0.040
	e (m)		0.005		0.060			0.240		0.080
	R ($K.m^2/W$)		0.071		0.043			0.114		2.000

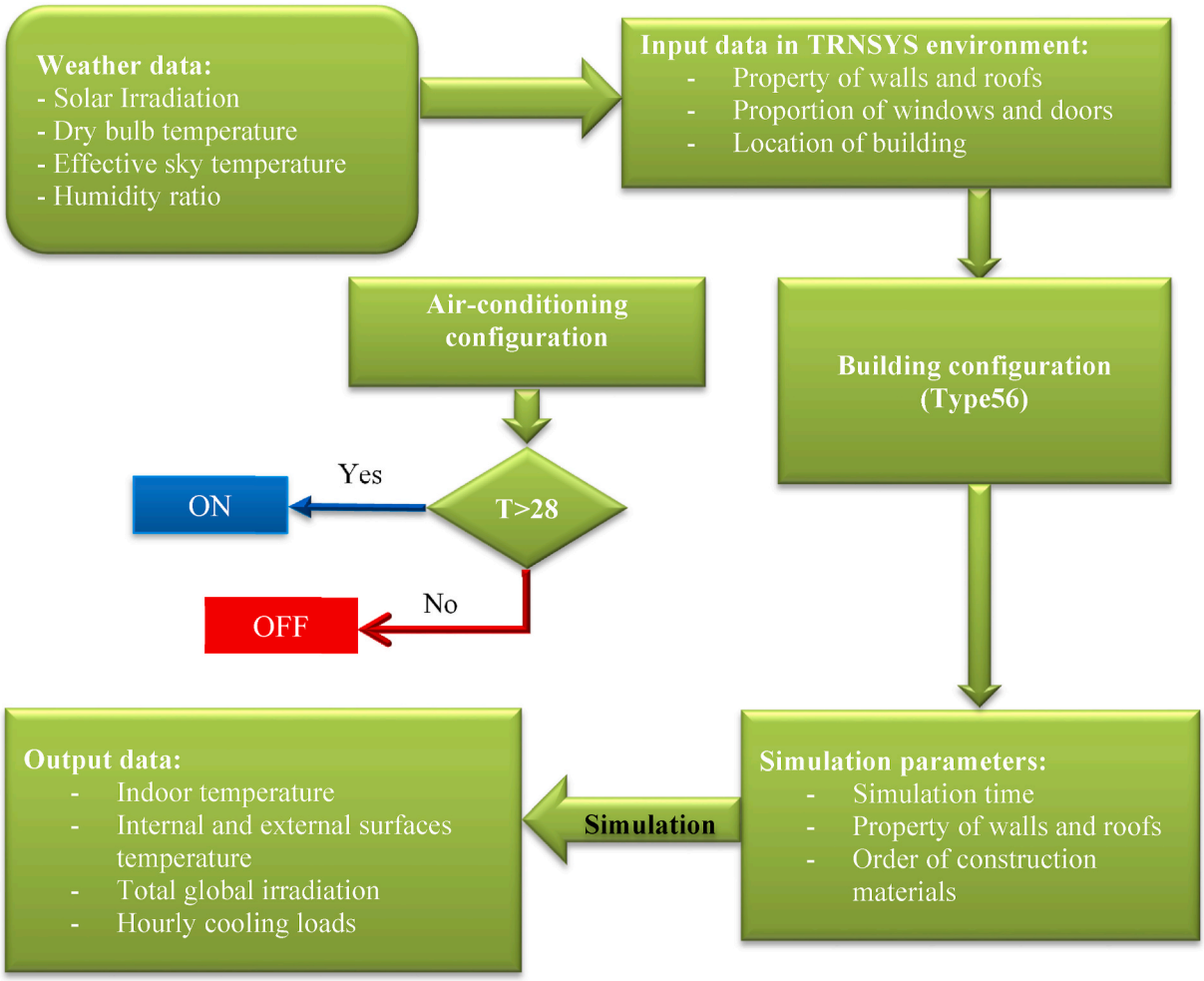

Fig. 6. Flowsheet for the simulation model developed with TRNSYS.

leading to the lower thermal conductivity was considered for both DPF (1.32% in wt.; λ = 0.381 W/m.K), and DPS (1.36% in wt.; λ = 0.106 W/m.K).

The following design parameters and assumptions were considered:

- The rooms had the same external dimensions, i.e., 4 × 4 × 4 m^3.
- The window in the north façade of each room had external dimensions of 1 × 1 m^2.
- The door in the north façade of each room had external dimensions of 2 × 0.8 m^2.
- The rooms had no internal loads i.e., lighting, equipment, or occupants.

Table 3 shows the thermal characteristics of the materials used in each room. Fig. 6 presents the flowsheet for the simulation model developed in a TRNSYS environment.

3.2. Results and discussion

The daily temperature profiles of the ambient indoor, internal, and external surfaces of each wall and the roof of each one of the three rooms

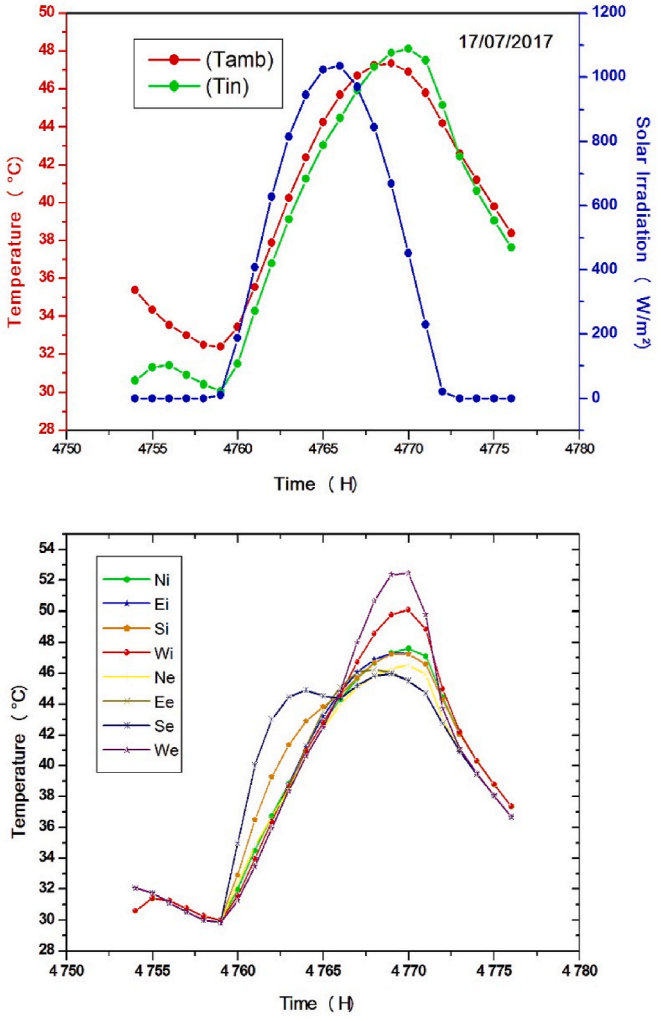

Fig. 7. Temperature profiles in room (a) on July 17th, 2017.

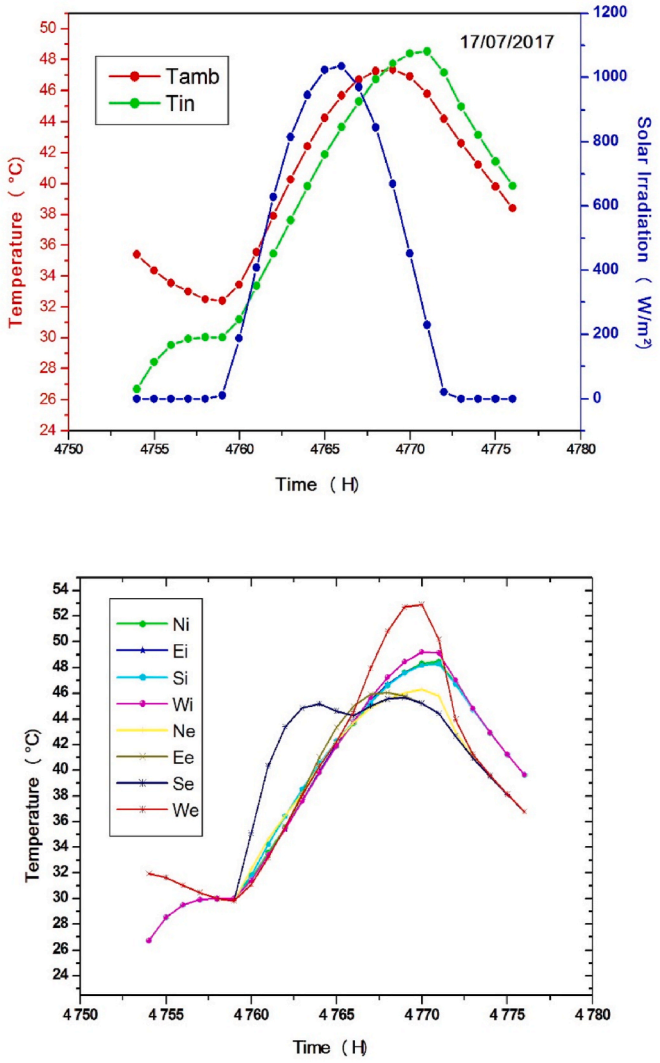

Fig. 8. Temperature profiles in room (b) on July 17th, 2017.

were established for a typical day in July on July 17th, as recommended by Duffie et al. [38]. Afterwards, the thermal insulation efficiency and electricity consumption during the summer period were estimated for each room. It is worthy of note, that the indoor temperature profile was determined with and without air-conditioning. The difference in the cost of the air-conditioning system in the three rooms was also analyzed. The results are discussed in the following sub-sections.

3.2.1. Temperature profiles in room (a)

Fig. 7 shows the solar irradiation and temperature profiles of ambient air, indoor air, and internal and external surfaces of the four walls i.e., East, West, North and South on July 17th, 2017. The indoor temperature was slightly lower than the ambient temperature except for a short period at mid-day where the tendency was the inverse. The maximum temperature difference during this short period was about 2 °C. As regards the temperature profiles of the internal and external surfaces of the East, West, North and South walls, it was apparent that the lowest temperature profile was that of the northern wall for which the peak temperature was 47.6 °C. The highest temperature profile was that of the western wall with a peak temperature of 52.5 °C. The temperature of the internal surfaces was significantly affected by the external temperature, which evidenced the weakness of the insulation system in that room compared to the other two rooms.

3.2.2. Temperature profiles in room (b)

On hot days, the indoor temperature, and the ambient air temperature at mid-day i.e., peak of solar irradiation reached 48.5 and 47.4 °C, respectively, as shown in Fig. 8. It is apparent that the external weather had no significant effect on the temperature of the internal surfaces of the wall, which justified the use of DPF for heat insulation purposes in buildings. Moreover, there was a period of high temperature in the afternoon, referred to as the "Thermal storage effect", which did not occur in the case of room (a) the one without heat insulation. It was also noticeable that at the beginning of the day, and up until mid-day, the indoor room temperature was lower than the outdoor temperature due to the heat insulation used. After that the indoor room temperature increased gradually until it exceeded the external air temperature. This in turn was due to the "Thermal storage effect" in the afternoon, brought about by the use of the heat insulator. Both temperature profiles converge towards the same value at sunset.

3.2.3. Temperature profiles in room (c)

In Fig. 9, the solar irradiation and temperature profiles of various components are depicted. These include the ambient air, indoor air, and the internal and external surfaces of the four walls: North, South East and West. By examining Fig. 9, we can observe how solar irradiation and temperature fluctuate throughout the day and across the different surfaces and environments within the room (c). This information is valuable for understanding the energy dynamics and thermal behavior within the room, aiding in the analysis and optimization of heating,

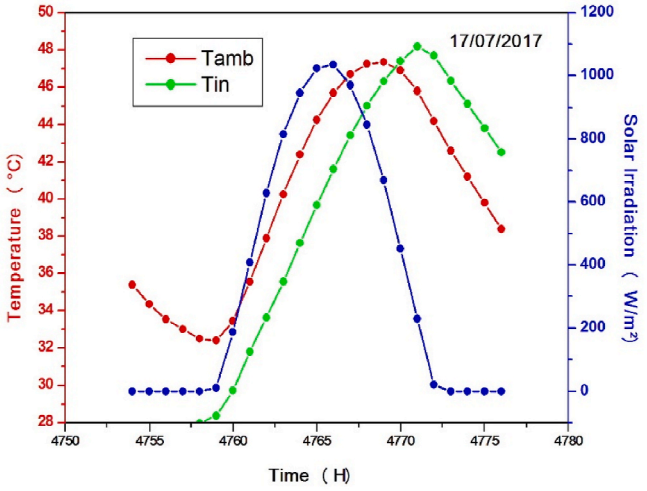

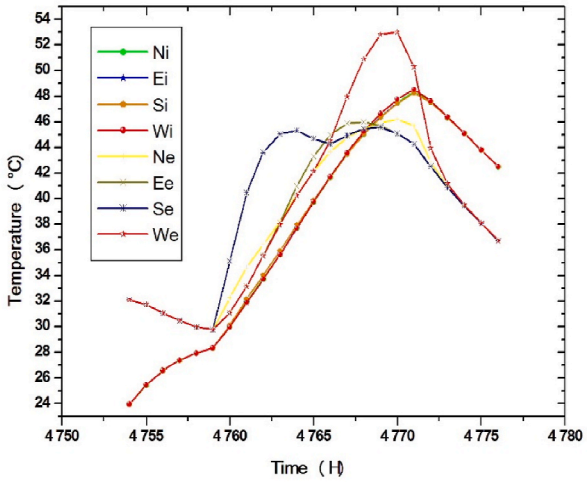

Fig. 9. Temperature profiles in room (c) on July 17th, 2017.

cooling, and insulation systems. The indoor temperature stayed at an almost constant value of 30 °C from sunrise to mid-day and increased after mid-day to 39 °C because of the "Thermal storage effect" caused by the heat insulation system. Also, the indoor temperature stayed around 2 °C below the outside temperature until mid-day, which indicated that heat insulation in room (c) was better than in rooms (a) and (b). Afterwards, the indoor temperature increased gradually until it exceeded the external temperature and remained relatively high at sunset again due to the "Thermal storage effect". This is not observed in the case of rooms (a) and (b). The maximum external wall surface temperature in the west wall was 52.9 °C. The insulation system used in room (c) allowed for the decrease of its indoor temperature during the day. The surface temperature of the outside western wall gradually rose and reached its highest value of 53 °C at 3 p.m. This was due to the scorching solar rays to which the outer walls are exposed. Then, the temperature gradually decreased and stabilized at 36 °C at sunset. It is also perceptible that the temperature of the internal surfaces was not significantly affected by the ambient temperature, which indicates that the thermal insulation system in room (c) was more effective than that of the other two rooms.

3.2.4. Temperature profiles of the internal and external surfaces of the room roofs

Fig. 10 shows the hourly variation of roof temperature i.e., underroof surface and on roof surface and solar irradiation. The external

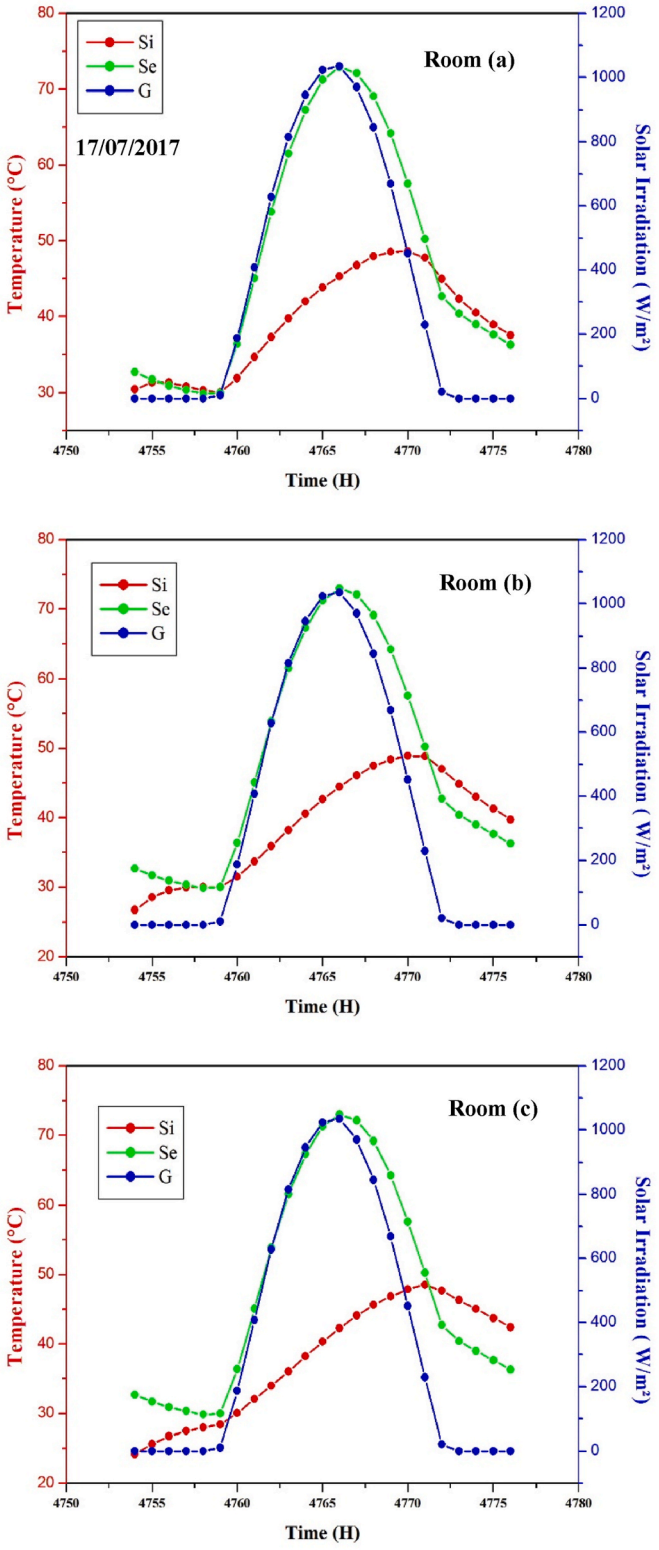

Fig. 10. Hourly variation of the internal and external temperatures in the room roofs on July 17th, 2017.

roof temperature was typically 6–28 °C higher than the internal roof temperature. The external surface temperature increased accordingly with the increase in solar radiation, while the internal surface temperature variation was much less pronounced with a moderate maximum temperature. The lowest internal roof temperatures recorded are 30.4 °C, 26.7 °C, and 24.2 °C for rooms (a), (b), and (c), respectively, on

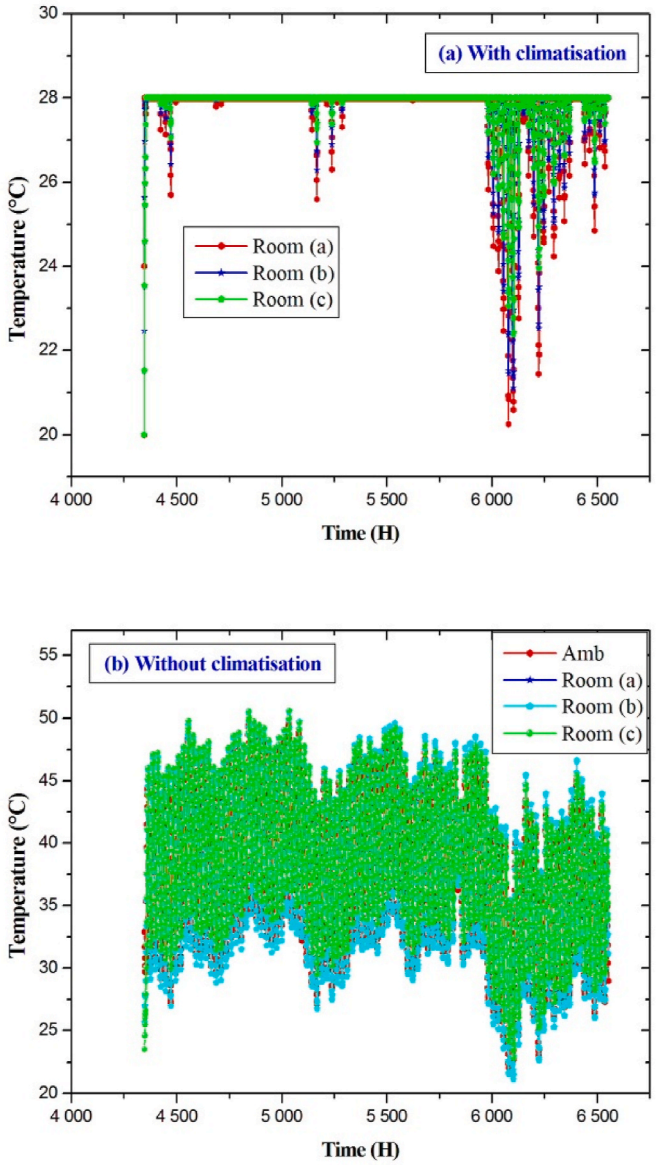

Fig. 11. Monthly variation of indoor temperature in the rooms: (a) With air-conditioning; (b) Without air-conditioning.

July 17th, 2017.

3.2.5. *Monthly variation of indoor temperature in the rooms*

Fig. 11 presents the monthly variation of indoor air temperatures in the rooms. These were calculated with and without air-conditioning supply systems during the summer months of July, August, and September. The air-conditioning system switches ON automatically when the indoor temperature exceeds 28 °C. The heat transfer process in room (c) is slower than that of the other two rooms, due to the high insulation provided by DPS. However, at the end of the day the indoor temperature in room (c) was higher than in the other rooms because of the insulation effect, which slowed down heat flow to the outside.

3.2.6. *Monthly variation of the hourly cooling loads in the rooms*

The hourly cooling loads in the rooms for the summer months of July, August, and September, are presented in Fig. 12. It is worthy of note, that no internal loads were considered for any of the rooms. The air-conditioning system switches ON automatically when the indoor temperature exceeds 28 °C. The total thermal energy demand for the three months was 2973.8, 1750.0 and 1049.1 kW respectively, for room

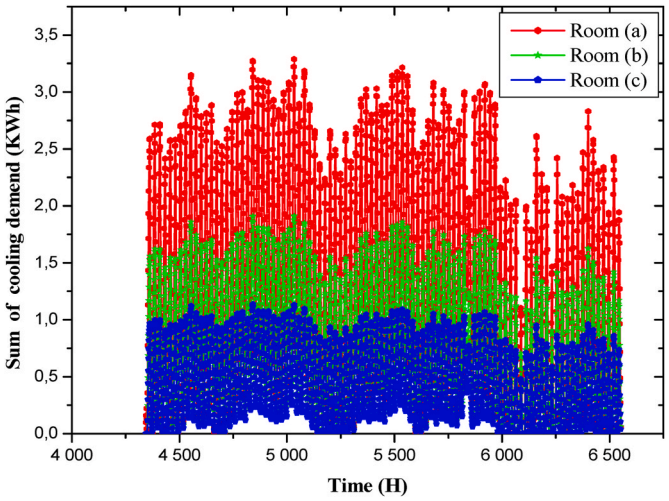

Fig. 12. Variation of the hourly cooling loads in rooms.

(a) built with sand and clay, room (b) which incorporated DPF, and room (c) which incorporated DPS. The use of clay and sand as building materials generates electricity consumption ranging from 1.5 to 3.4 kWh. This electricity consumption was between 1.0 and 1.8 when DPF was used as a heat insulator, and lower than 1 kWh in the case of DPS. This proves the effectiveness of using palm spikelet as a heat insulator as an alternative to the other materials used in this investigation. In comparison with the electricity demand for room (a) room (c) saw a reduction of 64.7% by adding DPS, and for room (b), with the addition of DPF, the electricity saving was around 41.2%.

4. Theoretical and experimental results of date palm wastes used for roof insulation in arid climates

The aim of this last section is to investigate the thermal insulation effect in roofs depending on the use of the material. Four different types of material were appraised namely polystyrene, air-gap, DPF and DPP. A prototype was built up for the experiment, consisting of 4 models of rooms. Each room had a different roof made from one of the types of material cited above. The experiments were conducted on three days, namely May 28th, 2016, October 16th, 2016, and May 25th, 2017. On each day, two materials were tested for two different rooms. The results were analyzed in terms of the solar irradiation and temperature profiles of external ambient air, indoor air, external and internal roof surfaces.

Envelope type insulation can play an important role in achieving energy-efficiency and low carbon emissions in buildings. The ideal insulation material is the one that has low thermal conductivity and high volumetric heat capacity. For regions requiring cooling, both properties are essential for achieving energy efficiency and comfort. In regions requiring heating however, lower thermal conductivity is of more importance as it hinders heat flow from indoors to outdoors [39].

4.1. *Description of the prototype*

The experimental setup consisted of two rooms with identical external dimensions, i.e., $0.8 \times 0.8 \times 0.6$ m^3. Four thermocouples were installed in each room, as shown in Fig. 13. The thermocouples were:

- K1 located outside the room to measure the outdoor ambient temperature.
- K2 located inside the room to measure the indoor temperature.
- K3 located on the external surface of the roof of the room.
- K4 located on the internal surface of the roof of the room.

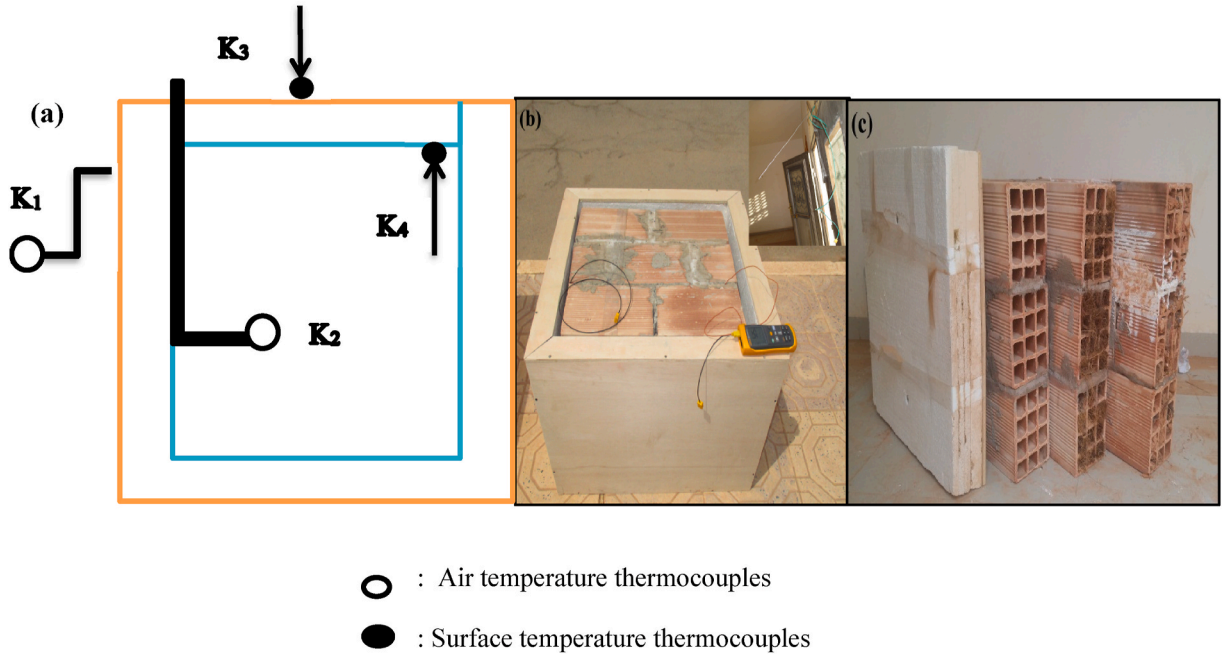

Fig. 13. Experimental prototype: (a) Thermocouple placement; (b) Measurement method; (c) Roofs used.

Table 4
Thermal characteristics of the materials used in each prototype.

	Unit	Prototype (a)	Prototype (b)	Prototype (c)	Prototype (d)
Roof	–	Polystyrene	Air gap brick	R_{DPF}	R_{DPP}
	λ (W/m. K)	2.880	2.510	1.690	4.260
	e (m)	0.10	0.15	0.15	0.15
	R ($K.m^2/W$)	0.035	0.060	0.089	0.035
Walls	λ (W/m. K)	2.880	2.880	2.880	2.880
	e (m)	0.10	0.10	0.10	0.10
	R ($K.m^2.W^{-1}$)	0.035	0.035	0.035	0.035

4.2. Simulation approach

The simulation tool developed in the present work is based on a mathematical model that uses the equations of energy balance and of heat transfer by conduction, convection, and radiation. The data from experimentally determined thermal conductivity was used in the model as an input parameter. The thermal conductivity of each material used in this investigation was determined from the equations described below. Moreover, on the three-days experiment, internal and external roof surface temperatures were taken to register the difference between them, and establish time stability (or steady state mode). The metrological data used in the simulation were obtained from Meteonorm V7.13 software, type TM2 [40]. And TRNSYS simulation was used. Thermal characteristics of the materials used in each prototype are summarized in Table 4.

Heat flux was determined applying the flowing equation:

$$\varphi_{con} = \varphi_{cnv} + \varphi_r \tag{3}$$

Where:

$$\varphi_{cnv} = H \times \delta T = H \times \left(T_{sky} - T_{Amb}\right) \tag{4}$$

H = 25, this value was reported in a technical document of the Algerian Ministry of Building and Urbanism [41].

The sky temperature was calculated applying the flowing equation [42]:

$$T_{sky} = 0.0552 \times T_{amb}^{1.5} \tag{5}$$

$$\varphi_r = I * C_a \tag{6}$$

I was taken from the Algerian National Weather Office (2017) [43].
C_a = 0.70, this value was reported by CNERIB [41].
Thermal conductivity was calculated as follow [44]:

$$\varphi_{con} = \frac{\lambda * e}{(T_{se} - T_{si})} \tag{7}$$

$$\lambda = \frac{\varphi_{con} * e}{(T_{se} - T_{si})} \tag{8}$$

4.3. Comparison between theoretical and experimental results

4.3.1. Outdoor temperature and solar irradiation

The experimental results of ambient temperature and solar irradiation are compared with those obtained by simulation in Fig. 14 for three different days in the summer period, namely May 28th, 2016, October 16th, 2016, and May 25th, 2017. The data obtained on May 28th, 2016, was well in accordance with the data obtained from the experimental results and those of the simulation work. The maximum deviation for solar radiation was 380 W/m^2 at 16 h, while the maximum deviation for ambient temperature was 5.3 °C at 13 h. The remaining two days also showed that, solar radiation data for experimental and simulated values were also well in agreement. However, a significant increase in simulated ambient temperature was perceived after noon, because Meteonorm [40] calculates average temperature data over a 10-year period. The average deviation between the experimental and simulated data was around 34.0% and 7.6% respectively for solar radiation and ambient temperature.

4.3.2. Internal and external roof surface temperature profiles

Fig. 15 shows the experimental and simulated temperature profiles

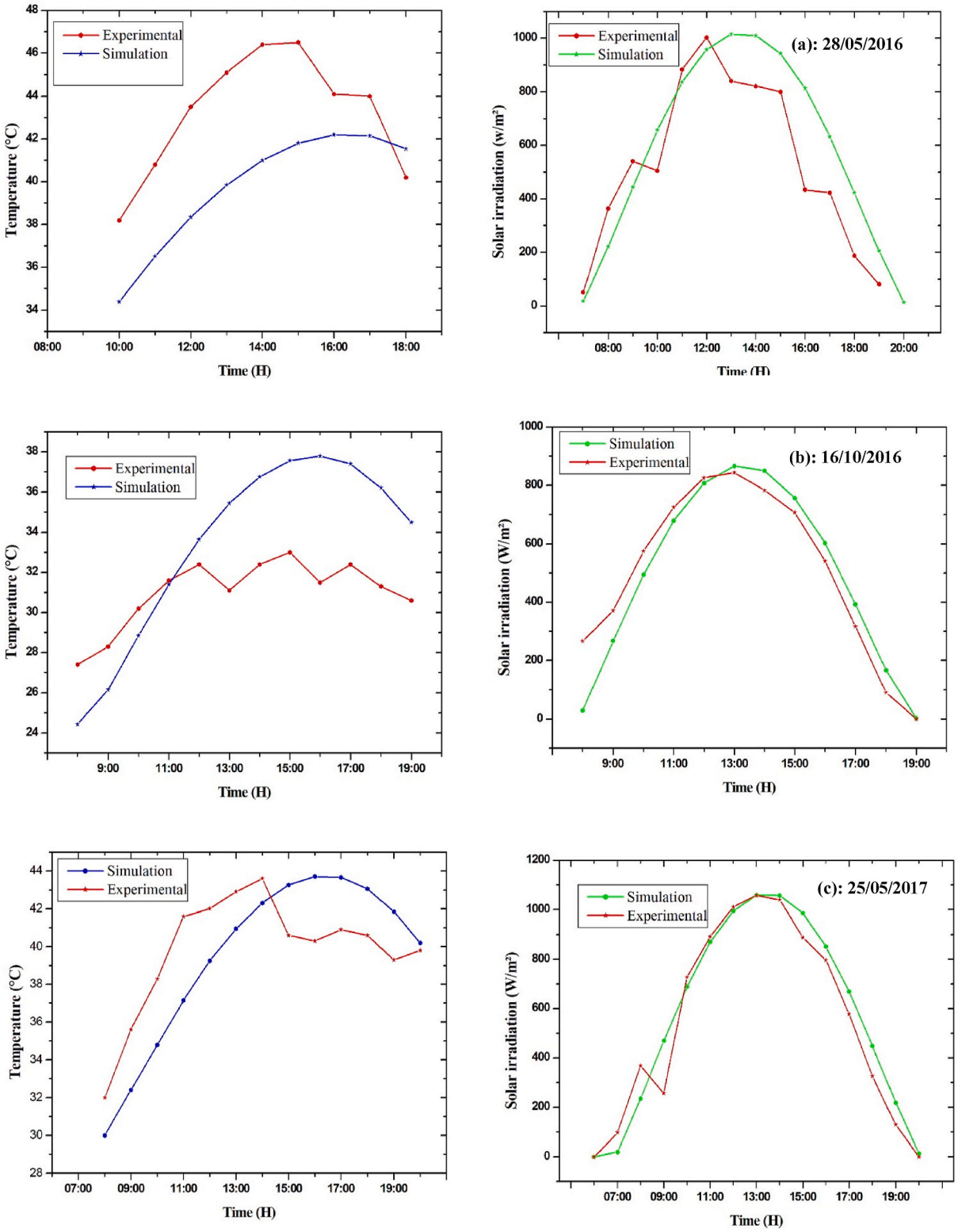

Fig. 14. Profiles of outdoor temperature and solar irradiation: (a) May 28th, 2016; (b) October 16th, 2016; (c) May 25th, 2017.

of the external and internal roof surfaces composed of different materials for the same three summer days considered above. In the data from October 16th, 2016, the use of DPF was seen to be more effective than the other insulation materials i.e., Polystyrene and DPP. The temperature difference between the external and internal roof surfaces reached 30.1 °C with the DPF roof, 24.8 °C and 11.5 °C with the polystyrene and DPP roofs, respectively. The use of DPP material reduced the temperature of the internal roof surface to 19.3 °C as can be seen in the data collected on May 25th. In the case of the bricks with air gaps, the temperature decreased to 14.3 °C. The use of polystyrene brought about a temperature decrease to 19.3 °C in the internal roof surface. It is worthy of note that the roof composed of DPF was more effective than the roofs composed of the other insulation materials, i.e., polystyrene and DPP.

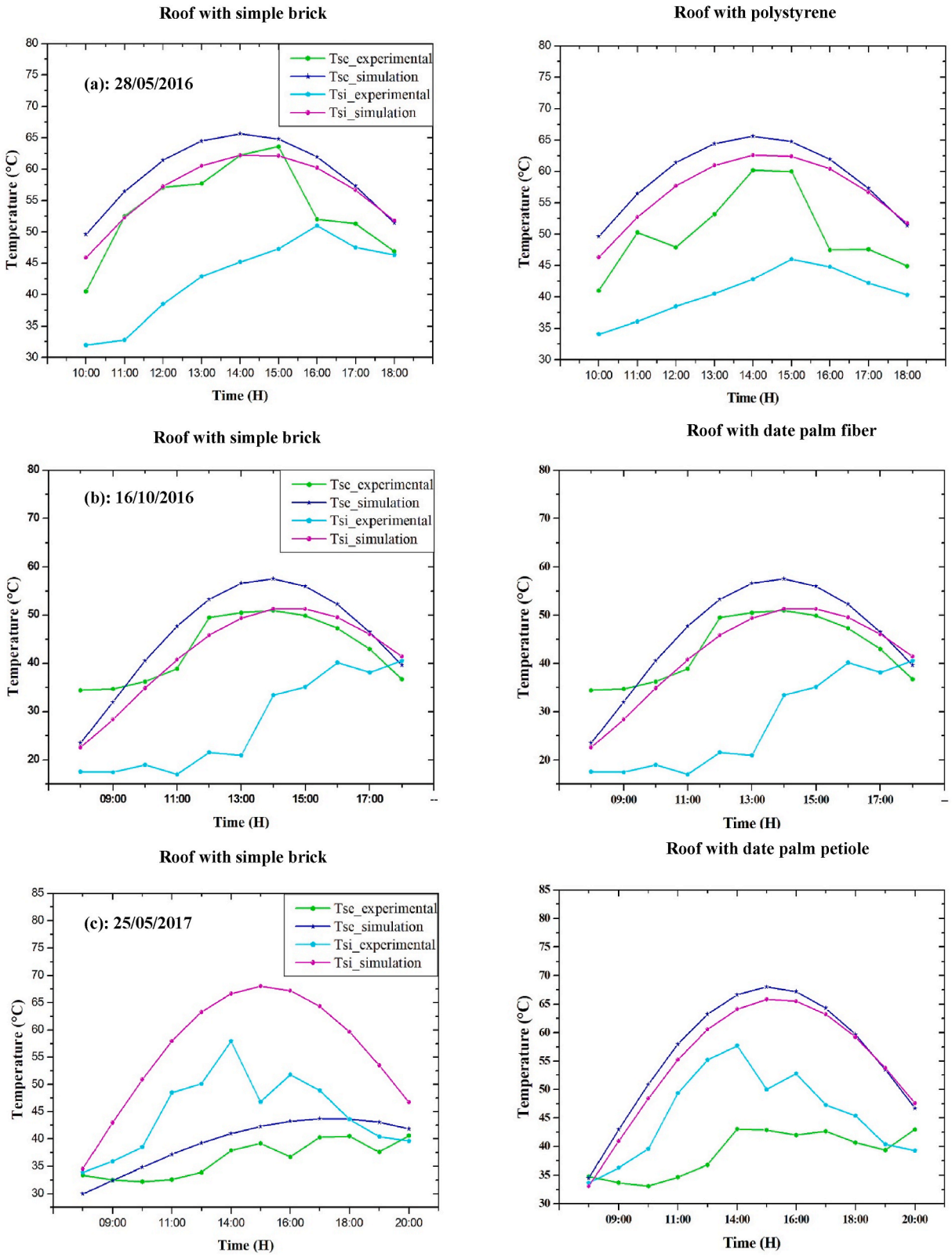

Fig. 15. Temperature profiles of external and internal roof surfaces: (a) May 28th, 2016; (b) October 16th, 2016; (c) May 25th, 2017.

4.3.3. Indoor temperature profile

Fig. 16 shows the variations in indoor temperature registered for the rooms using the thermal insulation materials examined in this investigation on the three days mentioned. As a thermal insulator, the DPF showed the best conditions for thermal comfort; polyester demonstrated the poorest conditions; while the DPP offered rather weak results. In the case of the roofs made with DPF, polyester, and DPP, indoor temperatures were 8.2, 5.0 and 4.5 °C, respectively, lower than the roof made of bricks. It is worthy of note that the indoor temperature was higher in the case of the roof made with DPF due to the "thermal storage effect"

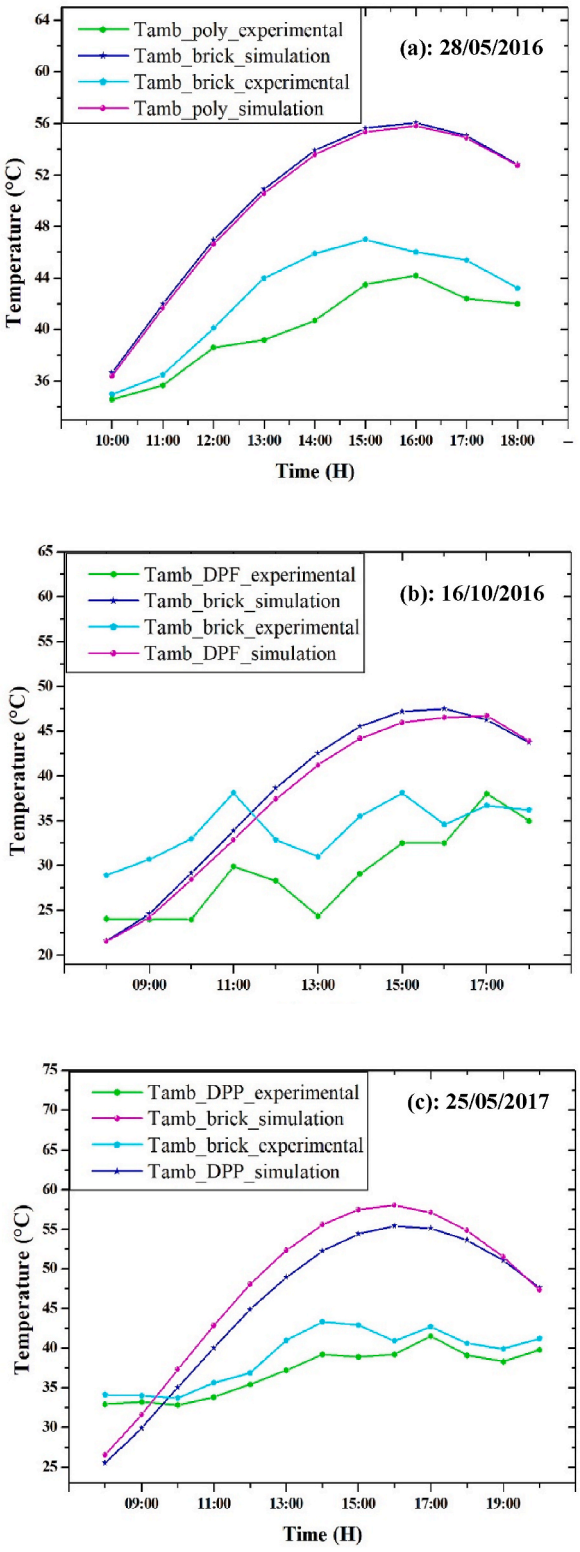

Fig. 16. Indoor temperature profiles for different roof materials on: (a) May 28th, 2016; (b) October 16th, 2016; (c) May 25th, 2017.

brought about by this material. The use of heat insulation materials in the roof prevented heat from flowing out of the rooms, giving rise to the high room temperatures at the end of the day.

5. Conclusions

Literature in recent years, has reported on several investigations carried out into the energy consumption of residential buildings and new strategies for reducing this energy consumption and mitigating carbon emissions. Insulation materials are incorporated into construction materials with an aim to decreasing heating/cooling energy demands and improving indoor thermal comfort in buildings. This study, carried out in the township of Adrar, located in the southwest of Algeria investigated the impact on energy performance of using thermal insulation made from waste date palm matter in buildings. Climatic conditions were those characteristics of the area. In a previous experiment, the authors had determined the thermal conductivity of seven samples of bricks made from different materials and with different concentrations. Afterwards, an analysis into the thermal and energy characteristics of three samples of bricks was carried out. Three different types of rooms were appraised, each incorporating one of the best performing insulators already determined for use in walls and roofs. Numerous experiments were conducted to determine the optimal ratios of elements necessary to achieve the desired form and consistency in the material. The weights of "DPF" at 50 g, 75 g, and 100 g corresponded to weight percentages of 0.72%, 1.01%, and 1.32% respectively. Similarly, the weights of "DPS" at 50 g, 75 g, and 100 g represented weight percentages of 0.70%, 0.97%, and 1.36% respectively. These particular ratios yielded the most favorable outcomes. The thermal conductivity of the samples was experimentally evaluated, and it was observed that the sample containing DPS at a weight percentage of 1.36% exhibited the best insulation performance, with a thermal conductivity of 0.106 W/m. K.

For the experimental rooms, the walls and roofing were constructed using DPF, DPP, and DPS materials. Comparing these structures to conventional materials (Sand + Clay), it was found that the electricity consumption for cooling during the summer months of July, August, and September decreased by up to 64.7% and 41.2% respectively. Moreover, compared to other insulation materials such as polystyrene and DPP, the use of DPF demonstrated a superior effectiveness. DPF, as a natural insulation material, has the potential to contribute significantly to passive cooling in hot regions, thus leading to reduced energy consumption and lower carbon dioxide (CO_2) emissions.

Based on these findings, further investigation into the mechanical strength and durability of these materials is strongly recommended. Additionally, the use of scanning electron microscopy can help identify the factors contributing to the enhanced thermal insulation and the structural characteristics of the brick components. Emphasizing geometric form can also be beneficial in improving the overall performance of the materials.

Credit authors statement

Djamel Belatrache: Conceptualization, Methodology, Software, Validation, Formal analysis, Investigation, Writing - Original Draft.; Said Bentouba: Conceptualization, Methodology, Formal analysis, Writing - Review & Editing, Supervision, Project administration.; Nadjet Zioui: Conceptualization, Methodology, Writing - Review & Editing.; Mahmoud Bourouis: Conceptualization, Methodology, Formal analysis, Writing - Review & Editing, Supervision, Project administration.

Declaration of competing interest

The authors declare that they have no known competing financial interests or personal relationships that could have appeared to influence the work reported in this paper.

Data availability

Data will be made available on request.

Acknowledgements

Djamel Belatrache gratefully acknowledges the University of Adrar for funding his internships at Rovira i Virgili University of Tarragona (Spain).

References

[1] Bélaïd F, Youssef M. Environmental degradation, renewable and non-renewable electricity consumption, and economic growth. Assessing the evidence from Algeria. Energy Pol 2017;102:277–87.
[2] Mawardi I, Aprilia S, Faisal M, Ikramullah I, Rizal S. An investigation of thermal conductivity and sound absorption from binderless panels made of oil palm wood as bio-insulation materials. Res Eng 2022;13:100319.
[3] Braiek A, Karkri M, Adili A, Ibos L, Ben Nasrallah S. Estimation of the thermophysical properties of date palm fibers/gypsum composite for use as insulating materials in building. Energy Build 2017;140:268–79.
[4] Boukhattem L, Boumhaout M, Hamdi H, Benhamou B, Ait Nouh F. Moisture content influence on the thermal conductivity of insulating building materials made from date palm fibers mesh. Construct Build Mater 2017;148:811–23.
[5] Haba B, Agoudjil B, Boudenne A, Benzarti K. Hygric properties and thermal conductivity of a new insulation material for building based on date palm concrete. Construct Build Mater 2017;154:963–71.
[6] Abdelaziz S, Guessasma S, Bouaziz A, Hamzaoui R, Beaugrand J, Souid AA. Date palm spikelet in mortar: testing and modelling to reveal the mechanical performance. Construct Build Mater 2016;124:228–36.
[7] Mawardi I, Aprilia S, Faisal M, Ikramullah, Rizal S. Characterization of thermal bio-insulation materials based on oil palm wood: the effect of hybridization and particle size. Polymers 2021;13(19).
[8] Drochytka R, Dvorakova M, Hodna J. Performance evaluation and research of alternative thermal insulation based on waste polyester fibers. Procedia Eng 2017; 195:236–43.
[9] Awad S, Zhou Y, Katsou E, Yunfeng L, Mizi F. A critical review on date palm tree (phoenix dactylifera L.) fibres and their uses in bio-composites. Waste Biomass Valorization 2021;12:2853–87.
[10] Awad S, Hamouda T, Midani M, Zhou Y, Katsou E, Fan M. Date palm fiber geometry and its effect on the physical and mechanical properties of recycled polyvinyl chloride composite. Ind Crops Prod 2021;174:114172.
[11] Awad S, Hamouda T, Midani M, Katsou E, Fan M. Polylactic acid (PLA) reinforced with date palm sheath fiber bio-composites: evaluation of fiber density, geometry, and content on the physical and mechanical properties. J Nat Fibers 2023;20(1).
[12] Elseify LA, Midani M, Shihata LA, El-Mously H. Review on cellulosic fibers extracted from date palms (Phoenix Dactylifera L.) and their applications. Cellulose 2019;26:2209–32.
[13] Kuczyński T, Staszczuk A. Experimental study of the thermal behavior of PCM and heavy building envelope structures during summer in a temperate climate. Energy 2023:128033.
[14] Ng WL, Chin MY, Zhou J, Woon KS, Ching AY. The overlooked criteria in green building certification system: Embodied energy and thermal insulation on non-residential building with a case study in Malaysia. Energy 2022;259:124912.
[15] Damfeu JC, Meukam P, Jannot Y, Wati E. Modelling and experimental determination of thermal properties of local wet building materials. Energy Build 2017;135:109–18.
[16] Mastouri H, Benhamou B, Hamdi H, Mouyal E. Thermal performance assessment of passive techniques integrated into a residential building in semi-arid climate. Energy Build 2017;143:1–16.
[17] Korjenic A, Zach J, Hroudová J. The use of insulating materials based on natural fibers in combination with plant facades in building constructions. Energy Build 2016;116:45–58.
[18] Shin H, Kwak Y, Jo S-K, Kim S-H, Huh J-H. Development of an optimal mechanical ventilation system control strategy based on weather forecasting data for outdoor air cooling in livestock housing. Energy 2023;268:126649.
[19] Jiang W, Zhang K, Ma L, Liu B, Li Q, Li D, Qi H, Liu Y. Energy-saving retrofits of prefabricated house roof in severe cold area. Energy 2022;254:124455. Part C.
[20] Macintyre HL, Heaviside C. Potential benefits of cool roofs in reducing heat-related mortality during heatwaves in a European city, vol. 127. Environment International; 2019. p. 430–41.
[21] Mungur M, Poorun Y, Juggurnath D, Ruhomally YB, Rughooputh R, Dauhoo MZ, Khoodaruth A, Shamachurn H, Gooroochurn M, Boodia N, Chooneea M, Facknath S. A numerical and experimental investigation of the effectiveness of green roofs in tropical environments: the case study of Mauritius in mid and late winter. Energy 2020;202:117608.
[22] Abdelaziz S, Guessasma S, Bouaziz A, Hamzaoui R, Beaugrand J, Souid AA. Date palm spikelet in mortar: testing and modelling to reveal the mechanical performance. Construct Build Mater 2016;124:228–36.
[23] Stavrakakis GM, Androutsopoulos AV, Vyörykkä J. Experimental and numerical assessment of cool-roof impact on thermal and energy performance of a school building in Greece. Energy Build 2016;130:64–84.
[24] Qin Y, Zhang M, Hiller JE. Theoretical and experimental studies on the daily accumulative heat gain from cool roofs. Energy 2017;129:138–47.
[25] Suárez I, Prieto MM, Salgado I. Dynamic evaluation of the thermal inertia of a single-family house: scope of the retrofitting requirements to comply with Spanish regulations. Energy Build 2017;153:209–18.
[26] Brito Filho JP, Oliveira Santos TV. Thermal analysis of roofs with thermal insulation layer and reflective coatings in subtropical and equatorial climate regions in Brazil. Energy Build 2014;84:466–74.
[27] Vera S, Pinto C, Tabares-Velasco PC, Bustamante W, Victorero F, Gironás J, Bonilla CA. Influence of vegetation, substrate, and thermal insulation of an extensive vegetated roof on the thermal performance of retail stores in semiarid and marine climates. Energy Build 2017;146:312–21.
[28] Nocentini K, Achard P, Biwole P, Stipetic M. Hygro-thermal properties of silica aerogel blankets dried using microwave heating for building thermal insulation. Energy Build 2018;158:14–22.
[29] Kadri M, Bouchair A, Laafer A. The contribution of double skin roof coupled with thermo reflective paint to improve thermal and energy performance for the 'Mozabit' houses: case of Beni Isguen's Ksar in southern Algeria. Energy Build 2022;256:111746.
[30] Bovo M, Giani N, Barbaresi A, Mazzocchetti L, Barbaresi L, Giorgini L, Torreggiani D, Tassinari P. Contribution to thermal and acoustic characterization of corn cob for bio-based building insulation applications. Energy Build 2022;262: 111994.
[31] He Y, Lin ES, Tan CL, Tan PY, Wong NH. Quantitative evaluation of plant evapotranspiration effect for green roof in tropical area: a case study in Singapore. Energy Build 2021;241:110973.
[32] Ozarisoy B, Altan H. Systematic literature review of bioclimatic design elements: theories, methodologies and cases in the South-eastern Mediterranean climate. Energy Build 2021;250:111281.
[33] Lee J, Kim J, Song D, Kim J, Jang C. Impact of external insulation and internal thermal density upon energy consumption of buildings in a temperate climate with four distinct seasons. Renew Sustain Energy Rev 2017;75:1081–8.
[34] Belatrache D. Contribution à l'optimisation et l'amélioration de l'isolation d'une habitation utilisant une source renouvelable dans les zones arides. Ph.D Thesis. Algeria: University of Adrar; 2018.
[35] Marie I. Thermal conductivity of hybrid recycled aggregate–Rubberized concrete. Construct Build Mater 2017;133:516–24.
[36] Rashad M, Żabnieńska-Góra A, Norman L, Jouhara H. Analysis of energy demand in a residential building using TRNSYS. Energy 2022;254. Part B.
[37] Al-Saadi SN, Zhai ZJ. A new validated TRNSYS module for simulating latent heat storage walls. Energy Build 2015;109:274–90.
[38] Duffie JA, Beckman WA, Blair N. Solar engineering of thermal processes, photovoltaics, and wind. John Wiley & Sons; 2020. https://doi.org/10.1002/9781119540328.
[39] Kumar D, Alam PXWM, Zou JG, Sanjayan RA. Memon. Comparative analysis of building insulation material properties and performance. Renew Sustain Energy Rev 2020;131:110038.
[40] Remund J. Meteonorm: irradiation data for every place on Earth. https://meteonorm.com.
[41] DTR C3.4, Réglementaire Thermique des Bâtiments d'Habitation, Règles de Calcul des Apports Calorifiques des Bâtiments, Fascicule 2, Document Technique Réglementaire, ministère de l'Habitat et de l'Urbanisme. Alger: CNERIB; 2004.
[42] Bouadila S, Kooli S, Skouri S, Lazaar M, Farhat A. Improvement of the greenhouse climate using a solar air heater with latent storage energy. Energy 2014;64:663–72.
[43] Algerian national weather office. https://www.meteo.dz/.
[44] Cherki A, Remy B, Khabbazi A, Jannot Y, Baillis D. Experimental thermal properties characterization of insulating cork–gypsum composite. Construct Build Mater 2014;54:202–9.